Sustainable Cities and Society 65 (2021) 102571

Contents lists available at ScienceDirect

Sustainable Cities and Society

journal homepage: www.elsevier.com/locate/scs

A deep learning-based social distance monitoring framework for COVID-19

Imran Ahmed [a], Misbah Ahmad [a], Joel J.P.C. Rodrigues [b,c], Gwanggil Jeon [d,e,*], Sadia Din [f]

[a] Center of Excellence in Information Technology, Institute of Management Sciences, 1-A, Sector E-5, Phase VII, Hayatabad, Peshawar, Pakistan
[b] Post-Graduation Program in Electrical Engineering (PPGEE), Federal University of Piauí, Teresina 64049-550, Brazil
[c] Instituto de Telecomunicações, 1049-001 Lisbon, Portugal
[d] School of Electronic Engineering, Xidian University, Xi'an, 710071, China
[e] Department of Embedded Systems Engineering, Incheon National University, Incheon, South Korea
[f] Department of Information and Communication Engineering, Yeungnam University, South Korea

ARTICLE INFO

Keywords:
Deep learning
Social distancing
COVID-19
Transfer learning
Overhead view
Person detection
YOLOv3

ABSTRACT

The ongoing COVID-19 corona virus outbreak has caused a global disaster with its deadly spreading. Due to the absence of effective remedial agents and the shortage of immunizations against the virus, population vulnerability increases. In the current situation, as there are no vaccines available; therefore, social distancing is thought to be an adequate precaution (norm) against the spread of the pandemic virus. The risks of virus spread can be minimized by avoiding physical contact among people. The purpose of this work is, therefore, to provide a deep learning platform for social distance tracking using an overhead perspective. The framework uses the YOLOv3 object recognition paradigm to identify humans in video sequences. The transfer learning methodology is also implemented to increase the accuracy of the model. In this way, the detection algorithm uses a pre-trained algorithm that is connected to an extra trained layer using an overhead human data set. The detection model identifies peoples using detected bounding box information. Using the Euclidean distance, the detected bounding box centroid's pairwise distances of people are determined. To estimate social distance violations between people, we used an approximation of physical distance to pixel and set a threshold. A violation threshold is established to evaluate whether or not the distance value breaches the minimum social distance threshold. In addition, a tracking algorithm is used to detect individuals in video sequences such that the person who violates/crosses the social distance threshold is also being tracked. Experiments are carried out on different video sequences to test the efficiency of the model. Findings indicate that the developed framework successfully distinguishes individuals who walk too near and breaches/violates social distances; also, the transfer learning approach boosts the overall efficiency of the model. The accuracy of 92% and 98% achieved by the detection model without and with transfer learning, respectively. The tracking accuracy of the model is 95%.

1. Introduction

COVID-19 originated from Wuhan, China, has affected many countries worldwide since December 2019. On March 11, 2020, the World Health Organization (WHO) announced it a pandemic diseases as the virus spread through 114 countries, caused 4000 deaths and 118,000 active cases (WHO; W.H. Organization, 2020). On October 7, 2020, they reported more than 35,537,491 confirmed COVID-19 cases, including 1,042,798 deaths. The latest number of infected people due to pandemic is shown in Fig. 1 (W. C. D. C. Dashboard). Many healthcare organizations, scientists, and medical professionals are searching for proper vaccines and medicines to overcome this deadly virus, although no progress is reported to-date. To stop the virus spread, the global community is looking for alternate ways. The virus mainly spreads in those people; who are in close contact with each other (within 6 feet) for a long period. The virus spreads when an infected person sneezes, coughs, or talks, the droplets from their nose or mouth disperse through the air and affect nearby peoples. The droplets also transfer into the lungs through the respiratory system, where it starts killing lung cells. Recent studies show that individuals with no symptoms but are infected with the virus also play a part in the virus spread (W. C. D. C. Dashboard). Therefore, it is necessary to maintain at least 6 feet distance from others, even if people do not have any symptoms.

Social distancing associates with the measures that overcome the

* Corresponding author.
E-mail addresses: imran.ahmed@imsciences.edu.pk (I. Ahmed), misbahahmad4872@gmail.com, ms161605273@imsciences.edu.pk (M. Ahmad), joeljr@ieee.org (J.J.P.C. Rodrigues), gjeon@inu.ac.kr (G. Jeon), saadia.deen@gmail.com, sadiadin@yu.ac.kr (S. Din).

https://doi.org/10.1016/j.scs.2020.102571
Received 17 September 2020; Received in revised form 14 October 2020; Accepted 19 October 2020
Available online 1 November 2020

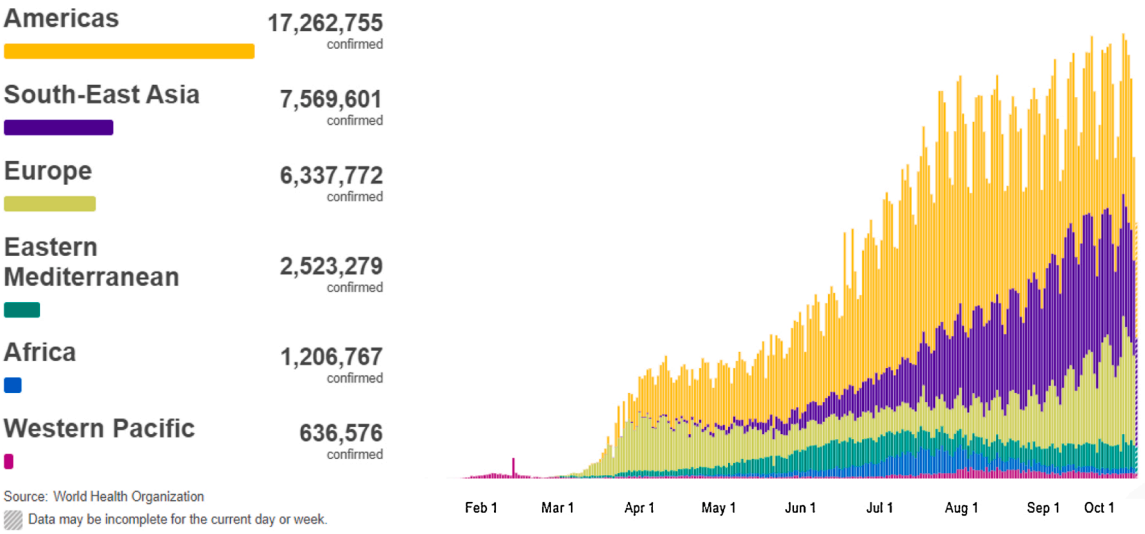

(a) Region wise number of confirmed cases (October 7, 2020)

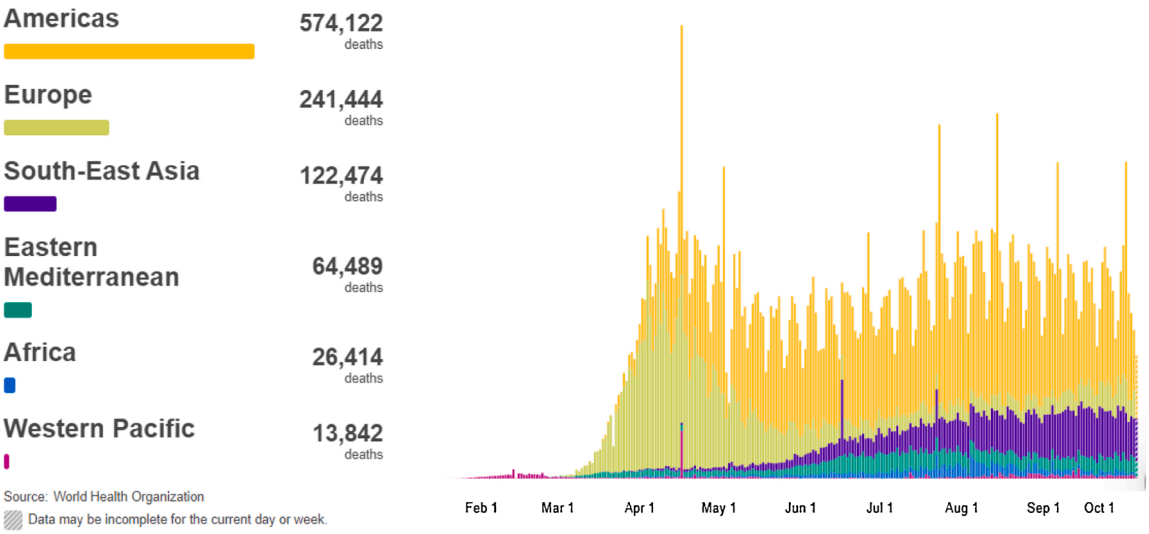

(b) Region wise number of deaths, (October 7, 2020).

Fig. 1. Latest number confirmed cases and deaths reported by WHO due to pandemic ().

virus' spread, by minimizing the physical contacts of humans, such as the masses at public places (e.g., shopping malls, parks, schools, universities, airports, workplaces), evading crowd gatherings, and maintaining an adequate distance between people (Adlhoch, 2020; Ferguson et al., 2005). Social distancing is essential, particularly for those people who are at higher risk of serious illness from COVID-19. By decreasing the risk of virus transmission from an infected person to a healthy, the virus' spread and disease severity can be significantly reduced (Statistica) Fig. 2. If social distancing is implemented at the initial stages, it can perform a pivotal role in overcoming the virus spread and preventing the pandemic disease's peak, as illustrated in Fig. 3 (Harvard). It can be observed that social distancing can decrease the number of infected patients and reduce the burden on healthcare organizations. It also lowers the mortality rates by assuring that the number of infected cases (patients) does not surpass the public healthcare capability (Nguyen et al., 2020).

In the past decades, computer vision, machine learning, and deep learning have shown promising results in several daily life problems. Recent improvement in deep learning allows object detection tasks (Brunetti, Buongiorno, Trotta, & Bevilacqua, 2018) more effective. Researchers (Punn, Sonbhadra, & Agarwal, 2020b; Ramadass, Arunachalam, & Sagayasree, 2020; Yang, Yurtsever, Renganathan, Redmill, & Özgüner, 2020), often utilize these methods to measure social distancing among people across the moving frames, as seen in Fig. 4. To determine the distancing between people, clustering and distance-based methods are utilized. From Fig. 4, it can be seen that most of the methods are developed using frontal or side view video sequences, which requires a proper camera calibration to map pixels to distance for real easily, measurable units (i.e., feet, meters, etc.). Secondly, if we assume a top-down approach, i.e., an overhead view approach, then the distance calculations from the overhead view will lead to a better distance approximation and wide coverage of the wide scene.

In this work, we used an overhead view to provide an effective framework for social distance monitoring. Some scholars, e.g. Ahmed

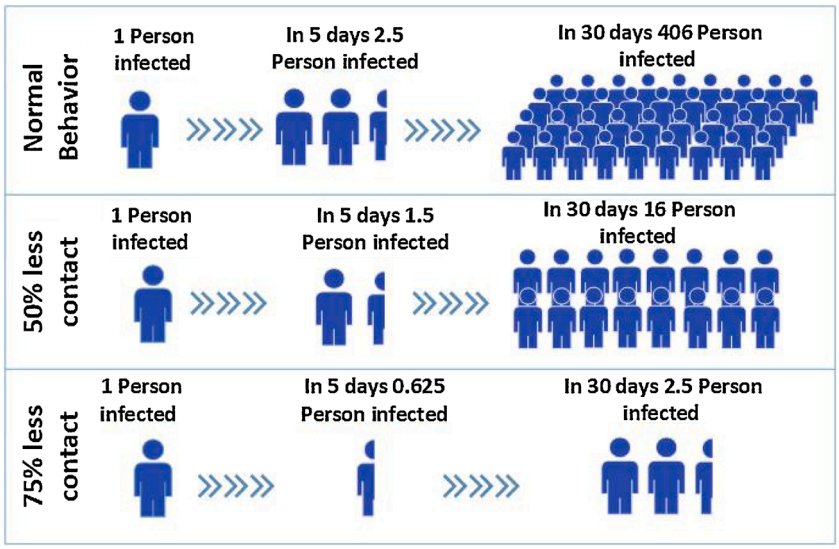

Fig. 2. Importance of social distancing.

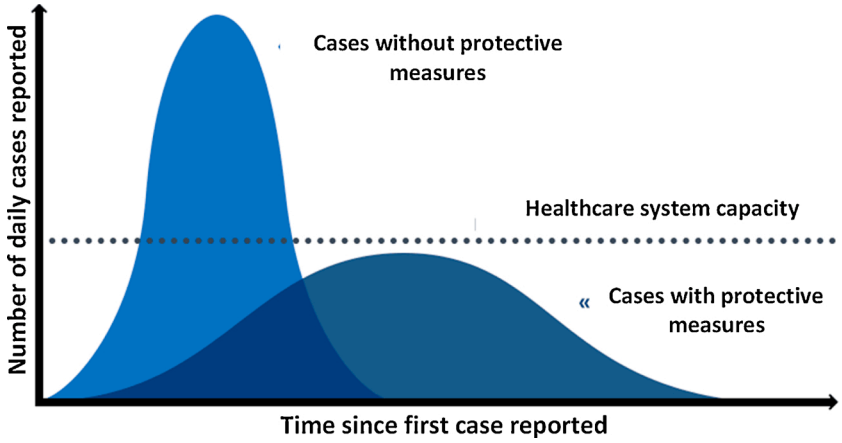

Fig. 3. Effect of social distancing: the peak of pandemic cases is decreasing and meeting with available healthcare capability ().

and Adnan (2017), Ahmad, Ahmed, Khan, Qayum, and Aljuaid (2020), Ahmed, Din, Jeon, and Piccialli (2019), Ahmed, Ahmad, Adnan, Ahmad, and Khan (2019), Ahmed, Ahmad, Piccialli, Sangaiah, and Jeon (2018), Ahmad, Ahmed, Ullah, Khan, and Adnan (2018), Choi, Moon, and Yoo (2015), and Migniot and Ababsa (2016) use an overhead perspective for human detection and tracking. The overhead perspective offers a better field of view and overcomes the issues of occlusion, thereby playing a key role in social distance monitoring to compute the distance between peoples. It might help overcome computation, communication load, energy consumption, human resource, and installation costs (Ahmad et al., 2019). This work aims to present a deep learning-based social distance monitoring framework for the public campus environment from an overhead perspective. A deep learning model, i.e., YOLOv3 (You Only Look Once) (Redmon & Farhadi, 2018), is applied for human detection. The current model (pre-trained on frontal or normal view data sets) is initially tested on the overhead data set. Transfer learning is also used to improve the efficiency of the detection model. To the best of our knowledge, this work could be considered as the first effort to use an overhead view perspective to monitor social distance with transfer learning. The detection model detects humans and gives bounding box information. After human detection, the Euclidean distance between each detected centroid pair is computed using the detected bounding box and its centroid information. A predefined minimum social distance violation threshold is specified using pixel to distance assumptions. To check, either the calculated distance comes under the violation set or not, the estimated information is matched with the violation threshold. The bounding box's color is formerly initialized as green; if the bounding box comes under the violation set, its color is updated to red. In addition, the centroid tracking algorithm is used to track a person who violated the social distancing threshold. The key goals of this work are as follows:

- To present a deep learning-based social distance monitoring framework using an overhead view perspective.
- To deploy pre-trained YOLOv3 for human detection and computing their bounding box centroid information. In addition, a transfer learning method is applied to enhance the performance of the model. The additional training is performed with overhead data set, and the newly trained layer is appended to the pre-trained model.
- In order to track the social distance between individuals, the Euclidean distance is used to approximate the distance between each pair of the centroid of the bounding box detected. In addition, a social distance violation threshold is specified using a pixel to distance estimation.
- Utilizing a centroid tracking algorithm to keep track of the person who violates the social distance threshold.
- To assess the performance of pre-trained YOLOv3 by evaluating it on an overhead data set. The output of the detection framework is assessed with and without the transfer learning. Furthermore, the

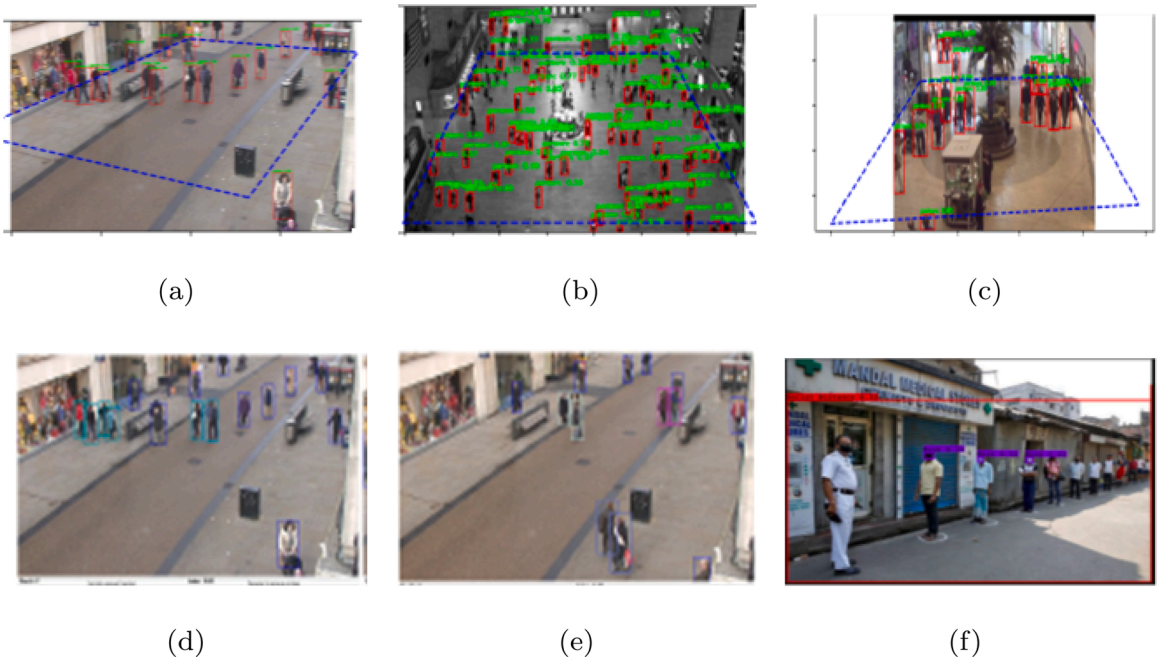

Fig. 4. Example images from the literature, used for social distance monitoring. (a), (b) and (c) Yang et al. (2020) used faster-RCNN for monitoring social distance. (d) and (e) Punn et al. (2020b) used YOLOv3 with Deepsort to monitor social distancing on Oxford Town Center, and (f) Ramadass et al. (2020).

model performance is also compared with other deep learning models.

The rest of the work discussed in the paper is structured as follows. The related work is presented in Section 2. A deep learning-based social distance monitoring framework has been presented in Section 3. The overhead view data set used for training and testing during experimentation is briefly discussed in Section 4. The detailed analysis of output results and performance evaluation of the model with and without transfer learning is also illustrated in this Section. The conclusion of the given work with potential future plans is provided in Section 5.

2. Literature review

After the rise of the COVID-19 pandemic since late December 2019, Social distancing is deemed to be an utmost reliable practice to prevent the contagious virus transmission and opted as standard practice on January 23, 2020 (B. News, 2020). During one month, the number of cases rises exceptionally, with two thousand to four thousand new confirmed cases reported per day in the first week of February 2020. Later, there has been a sign of relief for the first time for five successive days up to March 23, 2020, with no new confirmed cases (N. H. C. of the Peoples Republic of China, 2020). This is because of the social distance practice initiated in China and, latterly, adopted by worldwide to control COVID-19. Ainslie et al. (2020) investigated the relationship between the region's economic situation and the social distancing strictness. The study revealed that moderate stages of exercise could be allowed for evading a large outbreak. So far, many countries have used technology-based solutions (Punn, Sonbhadra, & Agarwal, 2020a) to overcome the pandemic loss. Several developed countries are employing GPS technology to monitor the movements of the infected and suspected individuals. Nguyen et al. (2020) provides a survey of different emerging technologies, including Wi-fi, Bluetooth, smartphones, and GPS, positioning (localization), computer vision, and deep learning that can play a crucial role in several practical social distancing scenarios. Some researchers utilize drones and other surveillance cameras to detect crowd gatherings (Harvey & LaPlace, 2019; Robakowska et al., 2017).

Until now researchers have done considerable work for detection (Iqbal, Ahmad, Bin, Khan, & Rodrigues, 2020; Patrick et al., 2020; Yash Chaudhary & Mehta, 2020), some provides an smart healthcare system for pandemic using Internet of Medical Things (Chakraborty, 2021; Chakraborty et al., 2021). Prem et al. (2020) studied the social distancing impacts on the spread of the COVID-19 outbreak. The studies concluded that the early and immediate practice of social distancing could gradually reduce the peak of the virus attack. As we all know, that although social distancing is crucial for flattening the infection curve, it is an economically unpleasant step. In Adolph, Amano, Bang-Jensen, Fullman, and Wilkerson (2020), Adolph et al. highlighted the United States of America's condition during the pandemic. Due to a lack of general support by decision-makers, it was not implemented at an initial stage, starting harm to public health. However, social distancing influenced economic productivity; even then, numerous scholars sought alternatives that overcame the loss.

Researchers provide effective solutions for social distance measuring using surveillance videos along with computer vision, machine learning, and deep learning-based approaches. Punn et al. (2020b) proposed a framework using the YOLOv3 model to detect humans and the Deepsort approach to track the detected people using bounding boxes and assigned IDs information. They used an open image data set (OID) repository, a frontal view data set. The authors also compared results with faster-RCNN and SSD. Ramadass et al. (2020) developed an autonomous drone-based model for social distance monitoring. They trained the YOLOv3 model with the custom data set. The data set is composed of frontal and side view images of limited people. The work is also extended for the monitoring of facial masks. The drone camera and the YOLOv3 algorithm help identify the social distance and monitor people from the side or frontal view in public wearing masks. Pouw, Toschi, van Schadewijk, and Corbetta (2020) suggested an efficient graph-based monitoring framework for physical distancing and crowd management. Sathyamoorthy, Patel, Savle, Paul, and Manocha (2020) performed human detection in a crowded situation. The model is designed for individuals who do not obey a social distance restriction, i.e., 6 feet of space between them. The authors used a mobile robot with an RGB-D camera and a 2-D lidar to make collision-free navigation in mass gatherings.

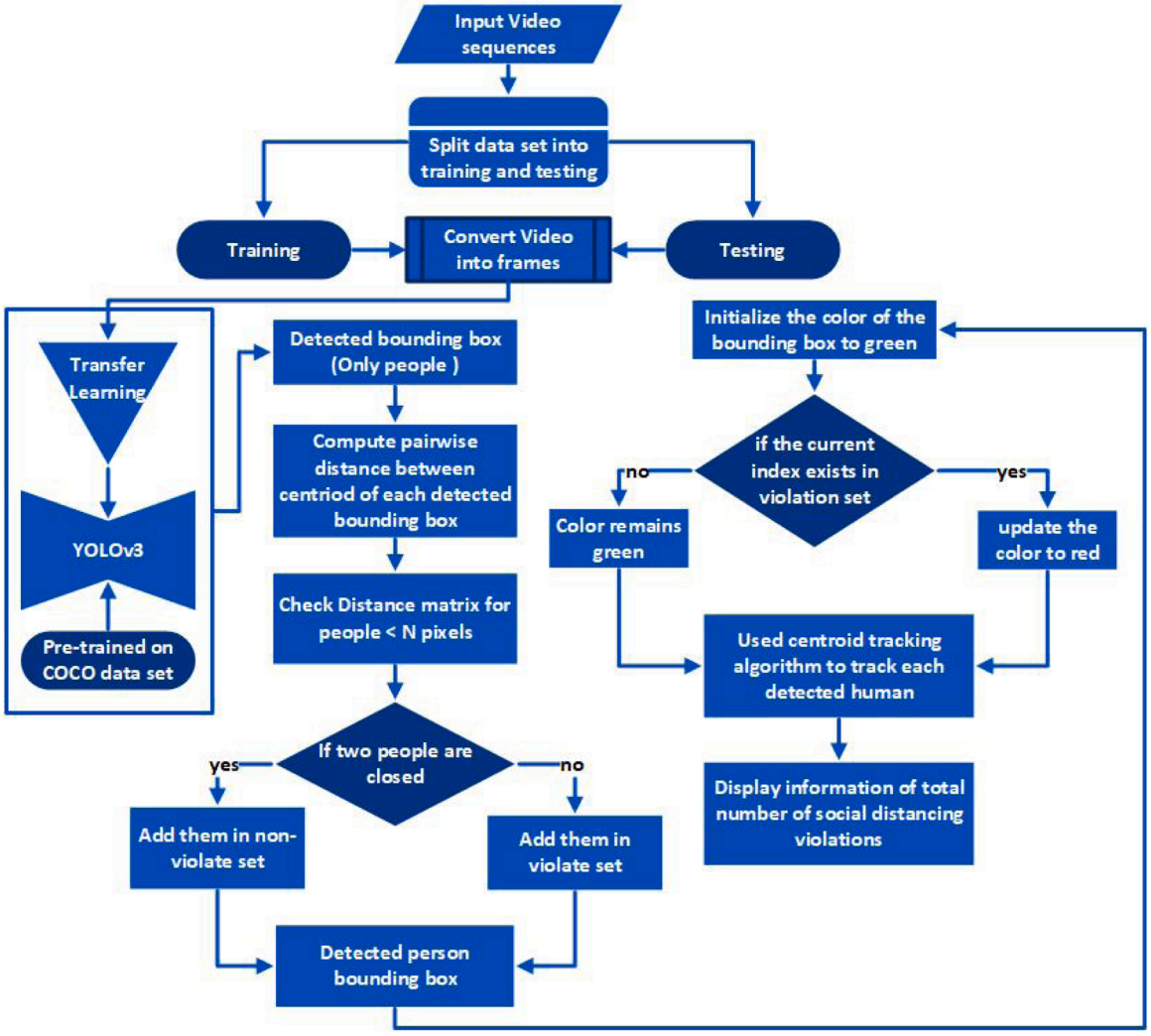

Fig. 5. Flow diagram of overhead view social distance monitoring framework.

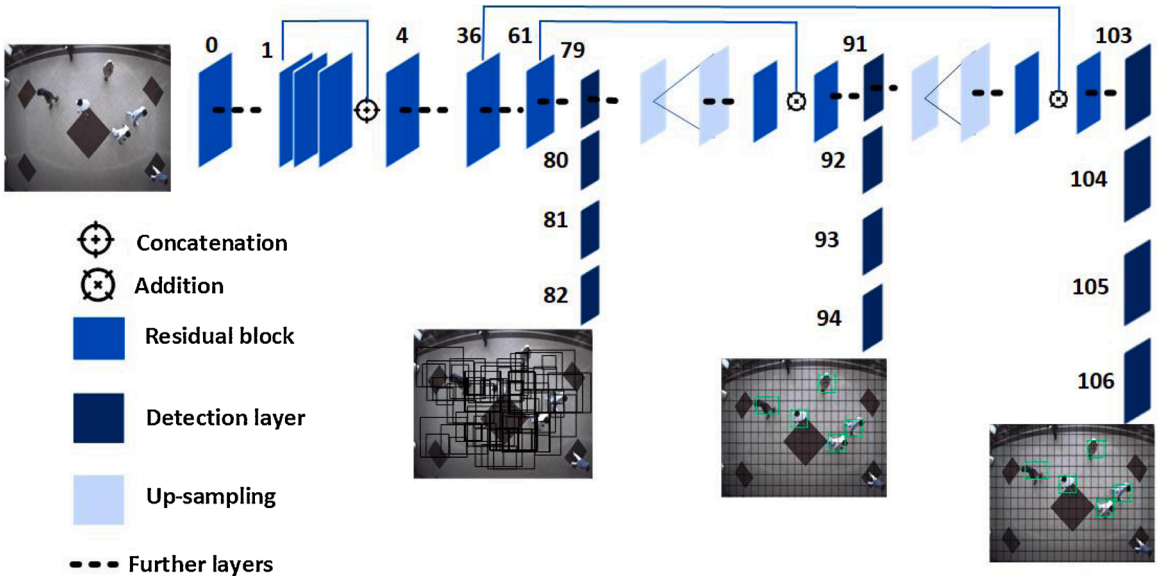

Fig. 6. General architecture of YOLOv3 utilized for overhead view human detection.

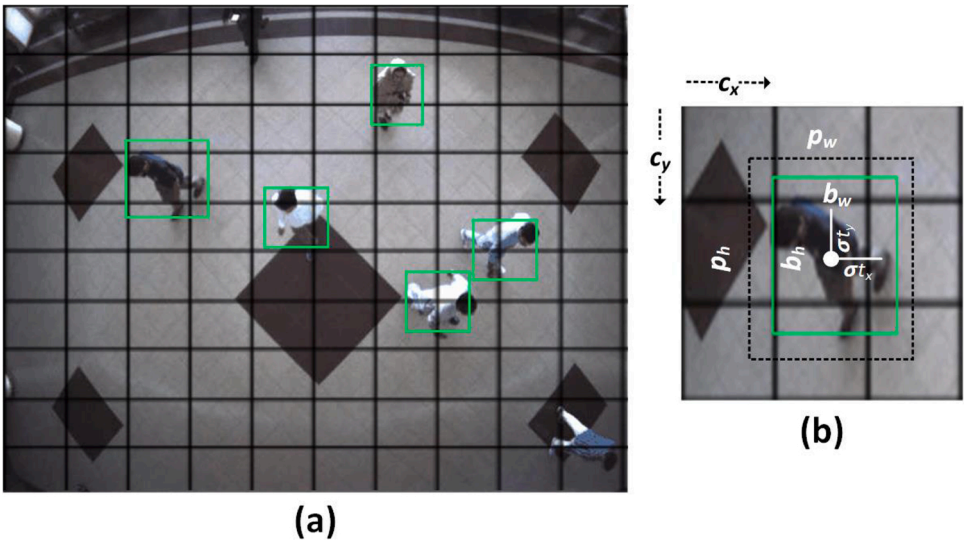

Fig. 7. Detected coordinates of person bounding box.

From the literature, we concluded that the researcher had done a considerable amount of work for monitoring of social distance in public environments. But, most of the work is focused on the frontal or side view camera perspective. Therefore, in this work, we presented an overhead view social distance monitoring framework that offers a better field of view and overcomes the issues of occlusion, thereby playing a key role in social distance monitoring to compute the distance between peoples.

3. Social distance monitoring

Researchers use a frontal or side perspective for social distance monitoring, as discussed in Section 22 . In this work, a deep learning-based social distance monitoring framework using an overhead perspective has been introduced. The flow diagram of the framework is shown in Fig. 5. The recorded overhead data set are split into training and testing sets. A deep learning-based detection paradigm is used to detect individuals in sequences. There are a variety of object detection models available, such as Krizhevsky, Sutskever, and Hinton (2012), Simonyan and Zisserman (2014), Girshick, Donahue, Darrell, and Malik (2014), Szegedy et al. (2015), Girshick (2015) and Ren, He, Girshick, and Sun (2015). Due to the best performance results for generic object detection, in this work, YOLOv3 (Redmon & Farhadi, 2018) is used. The model used single-stage network architecture to estimate the bounding boxes and class probabilities. The model was originally trained on the COCO (Common objects in context) data set (Lin et al., 2014). For overhead view person detection, transfer learning is implemented to enhance the detection model's efficiency, and a new layer of overhead training is added with the existing architecture.

After detection, the bounding box information, mainly centroid information, is used to compute each bounding box centroid distance. We used Euclidean distance and calculated the distance between each detected bounding box of peoples. Following computing centroid distance, a predefined threshold is used to check either the distance among any two bounding box centroids is less than the configured number of pixels or not. If two people are close to each other and the distance value violates the minimum social distance threshold. The bounding box information is stored in a violation set, as seen in Fig. 1, and the color of the bounding box is updated/changed to red. A centroid tracking algorithm is adopted for tracking so that it helps in tracking of those people who violate/breach the social distancing threshold. At the output, the model displays the information about the total number of social distancing violations along with detected people bounding boxes and centroids.

In this work, YOLOv3 is used for human detection as it improves predictive accuracy, particularly for small-scale objects. The main advantage is that it has adjusted network structure for multi-scale object detection. Furthermore, for object classification, it uses various independent logistic rather than softmax. The model's overall architecture is presented in Fig. 6; it can be seen that feature learning is performed using the convolutional layers, also called Residual Blocks. The blocks are made up of many convolutional layers and skip connections. The model's unique characteristic is that it performs detection at three separate scales, as depicted in Fig. 6.The convolutional layers with a given stride are practiced to downsample the feature map and transfer invariant-sized features (Redmon & Farhadi, 2018). Three feature maps, as shown in Fig. 6, are utilized for object detection.

The architecture shown in Fig. 6 is trained using an overhead data set. For that purpose, a transfer learning approach is adopted, that enhance the efficiency of the model. With transfer learning, the model is additionally trained without dropping the valuable information of the existing model. Further, the additional overhead data set trained layer is appended with the existing architecture. In this way, the model takes advantage of the pre-trained and newly trained information, and both detection results are further deliver better and faster detection results.

The architecture shown in Fig. 6 used a single-stage network for the entire input image to predict the bounding box and class probability of detected objects. For feature extraction, the architecture utilizes convolution layers, and for class prediction, fully connected layers are used. During human identification, as seen in Fig. 6, the input frame is divided into a region of $S \times S$, also called grid cells. These cells are related to bounding box estimation and class probabilities. It predicts the probability of whether the center of the person bounding box is in the grid cell or not:

$$\mathrm{Conf}(p) = \Pr(p) \times \mathrm{IOU}(\mathrm{pred}, \mathrm{actual}) \tag{1}$$

In Eq. (1), $\Pr(p)$ indicates that whether the person present is in the detected bounding box or not. The value of $\Pr(p)$ is 1 for yes and 0 for

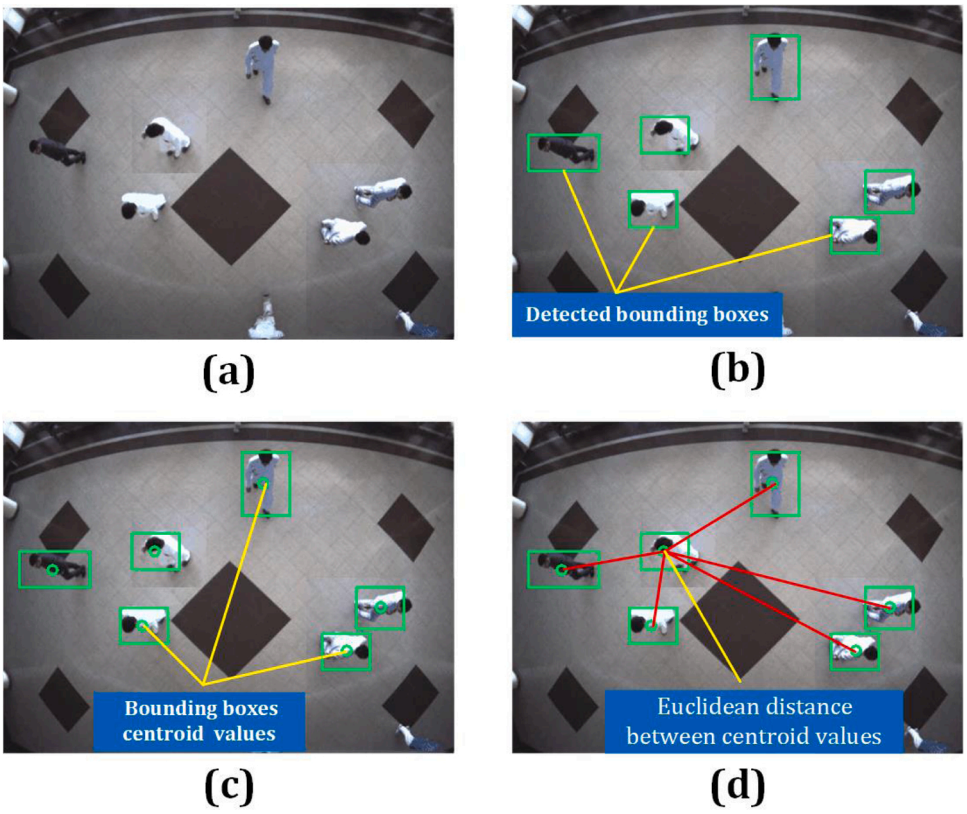

Fig. 8. (a) Input image, (b) detected person bounding boxes using deep learning algorithm, (c) compute the centroid of each detected bounding box, and (d) finally, the distance between each pair of the centroid is determined. In the example image, the red lines indicate the distance between each bounding box centroid. (For interpretation of the references to color in this figure legend, the reader is referred to the web version of this article.)

not. $\mathrm{IoU}(\mathrm{pred}, \mathrm{actual})$ determines the Intersection Over Union of the actual and predicted bounding box. It is defined as (Redmon & Farhadi, 2018):

$$\mathrm{IoU}(\mathrm{pred}, \mathrm{actual}) = \mathrm{area}\frac{\mathrm{BoxT} \cap \mathrm{BoxP}}{\mathrm{BoxT} \cup \mathrm{BoxP}} \tag{2}$$

where the ground truth box (actual) manually labeled in the training data set represented with BoxT, and the predicted bounding box is displayed as BoxP. area presents the area of intersection. An acceptable area is predicted and decided for each detected person in the input frame. The confidence value is applied after prediction to achieve the optimal bounding box. For each predicted bounding box, h, w, x, y are estimated, where bounding box coordinates are defined by x, y, and width and height are determined by w, h. The model produces the following predicted bounding box values as seen in Fig. 7 and Eq. (3) (Redmon & Farhadi, 2018);

$$\begin{aligned} b_x &= \sigma(t_x) + c_x \\ b_y &= \sigma(t_y) + c_y \\ b_w &= p_w e^{t}_{w} \\ b_h &= p_w h^{t}_{h} \end{aligned} \tag{3}$$

In Eq. (3), b_x, b_y, b_w, b_h are predicted coordinate bounding boxes, where the coordinates' center is represented as x, y and width and height with w, h. t_w, t_h, t_x, t_y, defined the network output and c_x, c_y are used to correspond the top-left coordinates of the grid cell as shown in Fig. 7, while the p_w and p_h are width and height of anchors.

A threshold value is defined that process the high confidence values and discards the low confidence values. Using non-maximal suppression, the final location parameters are derived for the detected bounding box. At last, loss function is calculated, for detected bounding box (Redmon & Farhadi, 2018). The given loss function is the sum of three functions, i.e., regression, classification, and confidence. At each grid cell, if the object is detected, then the classification loss is computed as the squared error of the conditional class probabilities and calculated as (Redmon & Farhadi, 2018);

$$\mathscr{L}_{\mathrm{cls}} = \sum_{i=0}^{S^2} 1_{\mathrm{ij}}^{\mathrm{obj}} \sum_{c \in \mathrm{class}} 1_{i}^{\mathrm{obj}} (p_i(c) - p*_i(c))^2 \tag{4}$$

In Eq. (4), in grid cell i if the person is detected then $1_{\mathrm{ij}}^{\mathrm{obj}} = 1$, otherwise equals to 0. The conditional class probabilities for class c in grid cell i are represented as $p*_i(c)$. The localization loss estimates the failures in the predicted bounding box sizes and locations. The bounding box containing the detected object, i.e., a person, is added. It is defined as (Redmon & Farhadi, 2018);

$$\begin{aligned} \mathscr{L}_{\mathrm{loc}} \quad &= \lambda_{\mathrm{coord}} 1_{\mathrm{ij}}^{\mathrm{obj}} \sum_{i=0}^{S^2} \sum_{j=0}^{B} [(x_i - x_i^*)^2 + (y_i - y_i^*)^2 \\ &\quad + (\sqrt{w_i} - \sqrt{w_i^*})^2 + (\sqrt{h_i} - \sqrt{h_i^*})^2] \end{aligned} \tag{5}$$

In above equation $1_{\mathrm{ij}}^{\mathrm{obj}}$ is equal to 1, in case if the jth bounding box in grid cell i is used for object detection, otherwise it is equal to 0. Instead of predicting simple height and width, the model predicts the square root of the bounding box width and height. In Eq. (5) the scale parameters λ_{coord} is used for predictions of bounding box coordinates and equals to 5 as (Redmon, Divvala, Girshick, & Farhadi, 2016). The predicted positions are represented with $x_i, \mathrm{yi}, h_i, w_i$ in ith cell of detected bounding box, while the actual positions of bounding box in the ith cell is defined using $x_i^*, y_i^*, h_i^*, w_i^*$. The Eq. (5) measures the loss function of predicted bounding box having coordinates value x, y. To represent the possibility

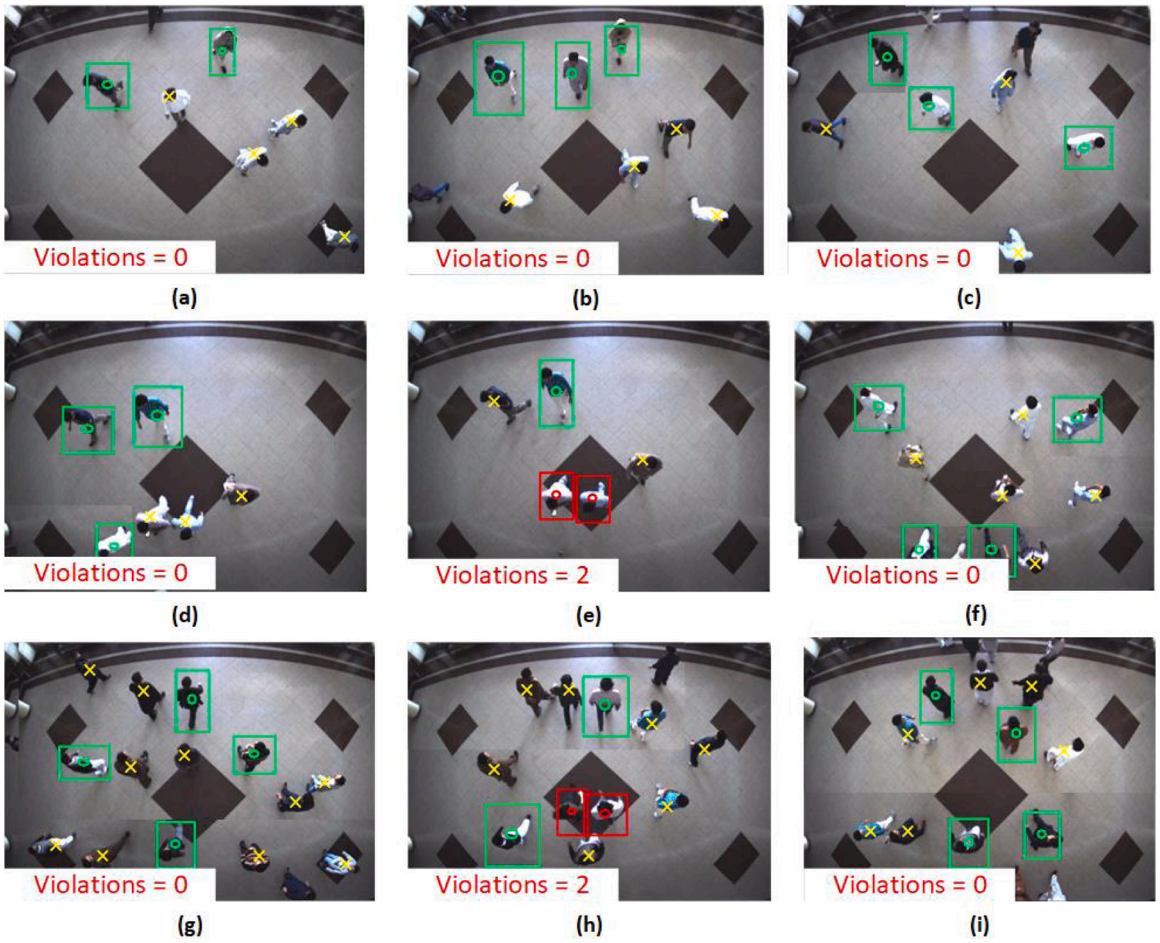

Fig. 9. Social distance monitoring from an overhead view using a pre-trained detection model. In sample frames, the people in green rectangles are those who maintain the social distancing. The people who violate the social distance threshold are shown red in rectangles. The manually labels yellow positive cross shows miss detections. (For interpretation of the references to color in this figure legend, the reader is referred to the web version of this article.)

of the detected person in the jth bounding box 1_{ij}^{obj} is used. The value of λ is constant, the function in Eq. (5) calculates sum over each bounding box, using ($j = 0$ to B) as predictor for each grid cell ($i = 0$ to S^2).

Finally the confidence loss is calculated that is given in Eq. (6) as (Redmon & Farhadi, 2018):

$$\mathscr{L}_{conf} = \sum_{i=0}^{S^2} \sum_{j=0}^{B} 1_{ij}^{obj} (C_i - C_i^*)^2 \tag{6}$$

where the confidence score is defined as C^*, for jth bounding box in grid cell i and 1_{ij}^{obj} and is equal to 1 in case if in cell i the jth bounding box is responsible for object detection; otherwise it is equal to 0. In case if the object is not detected, then the confidence loss is provided as (Redmon & Farhadi, 2018);

$$\mathscr{L}_{conf} = \lambda_{noobj} \sum_{i=0}^{S^2} \sum_{j=0}^{B} 1_{ij}^{noobj} (C_i - C_i^*)^2 \tag{7}$$

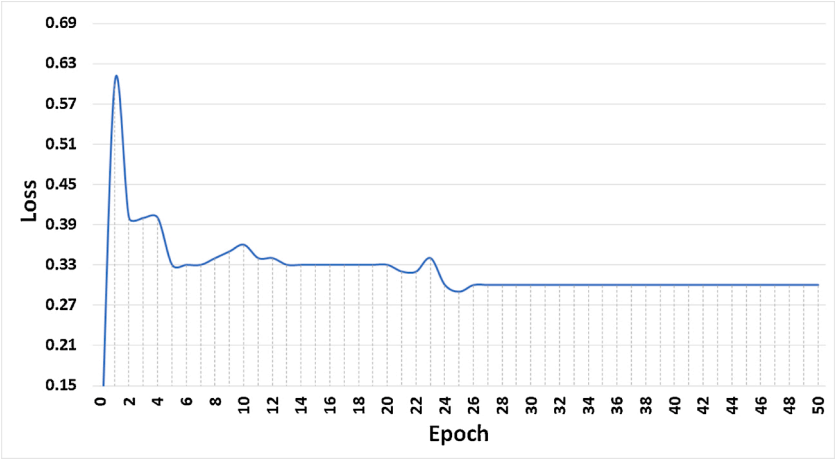

Fig. 10. Training loss of YOLOv3 using overhead view data set.

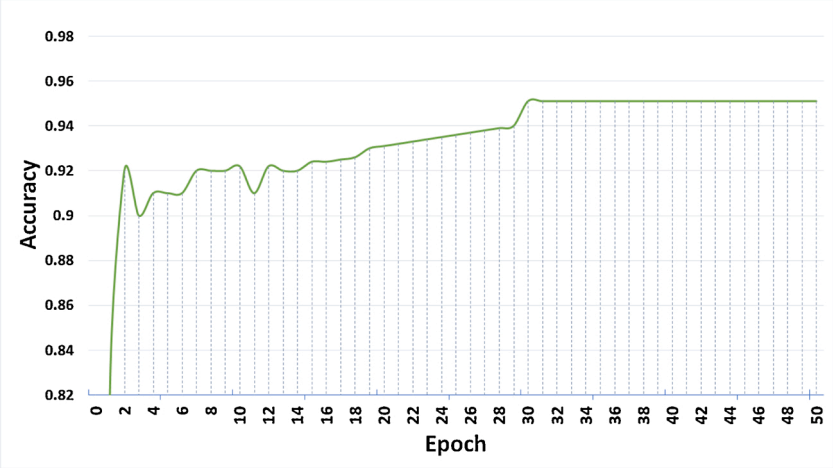

Fig. 11. Training Accuracy of YOLOv3 using overhead view data set.

In Eq. (7), 1_{ij}^{noobj} is defined as the complement of 1_{ij}^{obj}. The bounding box' confidence score C^* in cell i and λ_{noobj} is used to weights down the loss during detecting background. As in most cases detected, bounding boxes do not contain any objects that cause a class imbalance problem; therefore, the model is more frequently trained to detect background rather than detect objects. To solve this, the loss is weight down by a factor λ_{noobj} (default: 0.5).

After detecting people in video frames, in the next step, the centroid of each detected person bounding boxes shown as green boxes are used for distance calculation, as shown in Fig. 8(b). The detected bounding box coordinates (x, y) are used to compute the bounding box's centroid. Fig. 8(c) demonstrates accepting a set of bounding box coordinates and computing the centroid. After computing, centroid, a unique ID is assigned to each detected bounding box. In the next step, we measure

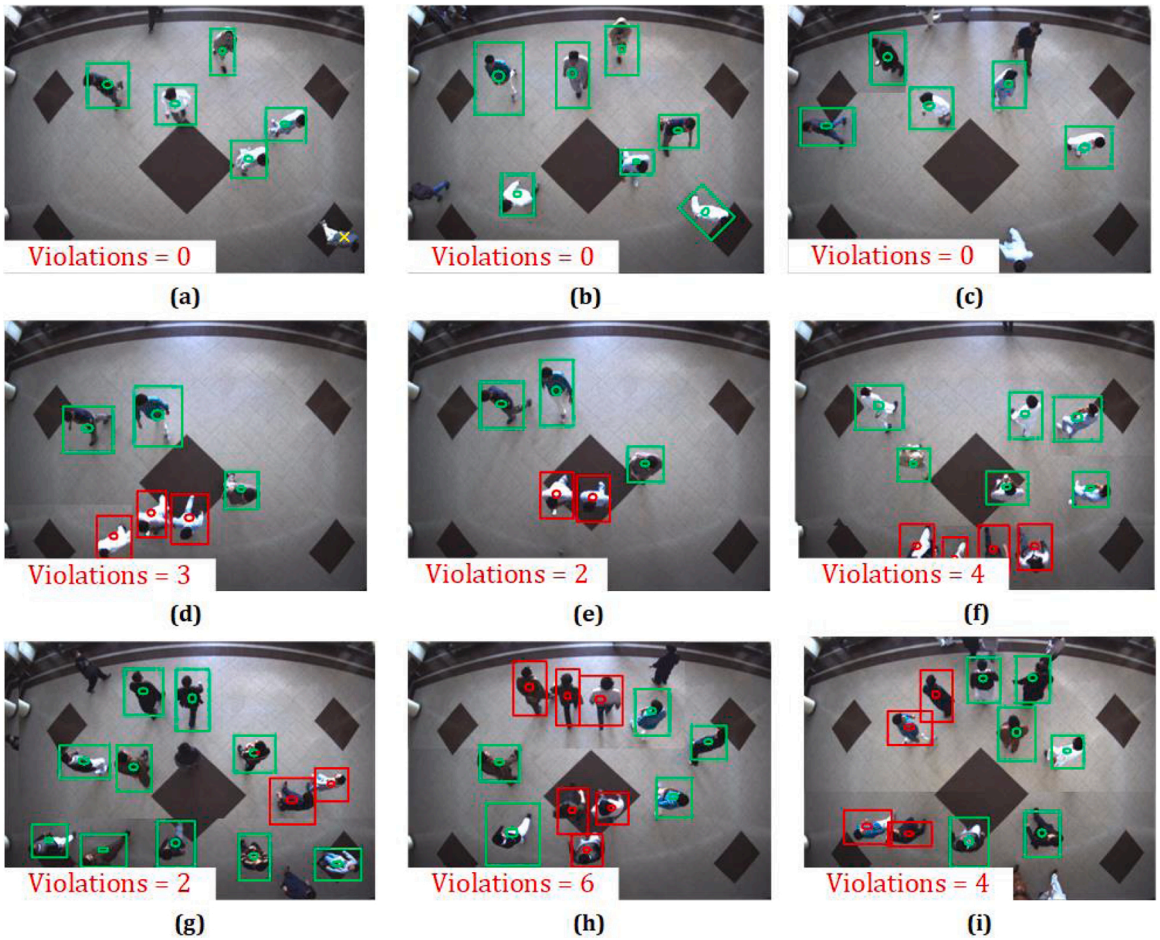

Fig. 12. Results of social distance monitoring, using transfer learning. It can be seen that the detection performance of the model is improved after transfer learning. In sample frames, the people in green rectangles maintain social distancing while in red rectangles are those who breach/violate the social distance. (For interpretation of the references to color in this figure legend, the reader is referred to the web version of this article.)

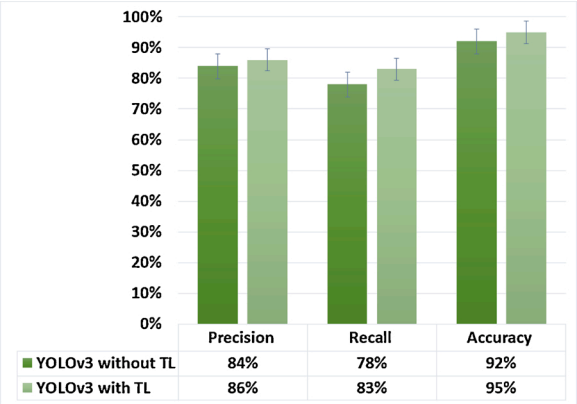

Fig. 13. Precision, Recall, and Accuracy of model (YOLOv3) with and without transfer learning.

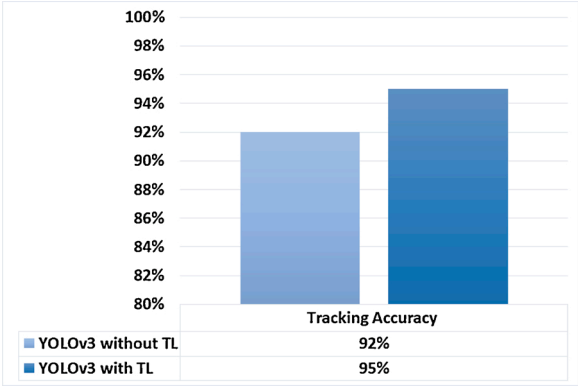

Fig. 14. Tracking accuracy with pre-trained and trained YOLOv3 detection model.

the distance between each detected centroid using Euclidean distance. For every subsequent frame in the video stream, we firstly compute bounding box centroids shown in Fig. 8(c); and then calculate the distance (highlighted with red lines) between each pair of detected bounding box centroids, Fig. 8(d). The information of each centroid is stored in the form of a list. Based on distance values, a threshold is defined to check if any two people are less than *N* pixels apart or not. If the distance violates the minimum social distance set or two people are too close, then the information is added into the violation set. The bounding box color is initialized as green. The information is checked in the violation set; if the current index exists violation set, the color is updated to red. Furthermore, the centroid tracking algorithm is used to track the detected people in the video sequence. The tracking algorithm also helps to keep track of people who are violating the social distance threshold. At the output, the model displays information about the total number of social distancing violations.

4. Experiments, results, and discussion

The detailed descriptions of various experiments carried out in this work are presented in this section. For social distance monitoring, an indoor data set recorded at Institute of Management Sciences, Hayatabad, Peshawar Pakistan is used (Ahmed, Ahmad, Adnan, et al., 2019; 2019a), containing video sequences captured from the overhead view. The data collection is divided into 70% and 30% training and testing, respectively. There is no restriction on the mobility of persons throughout the scene. Peoples in the scene move freely; their visual appearance is affected by radial distance and camera position. From example frames, it can be observed that the human's visual appearance is not identical, and peoples heights, poses, scales are varying in the data set. For implementation, we used OpenCV. The experimental results are divided into two subsections; first, the pre-trained model's testing results are discussed, while in the second subsection, the results of the detection model after applying transfer learning and training on the overhead data set are explained. For comparison, the model is tested using the same video sequences. The performance evaluation of the model is also made in this section, along with a comparison with different deep learning models.

4.1. Results of social distance monitoring using pre-trained model

In Fig. 9, the testing results of the social distance framework using a pre-trained model (Redmon & Farhadi, 2018) has been visualized. The testing results are evaluated using different video sequences. The people in the video sequences are freely moving in the scenes; it can be seen from sample frames that the individual's visual appearance is not identical to the frontal or side view (Fig. 9). The person's size is also varying at different locations, as shown in Fig. 9. Since the model only considers human (person) class; therefore, only an object having an appearance like a human is detected by a pre-trained model. The pre-trained model delivers good results and detects various size person bounding boxes, as shown with green rectangles in Fig. 9(a)–(c). From sample frames of Fig. 9, people are marked with green rectangles as they maintain a social distancing threshold. The model is also tested for multiple peoples, as depicted in Fig. 9(g)–(i), multiple people are entering in the scene. In sample images, it can be seen that after person detection, the distance between each detected bounding box is measured to check whether the person in the scene violates the social distance or not. In Fig. 9(e) and (h), two people at the center of the scene are marked with red bounding boxes as they violate or breaches the social distancing threshold. Some miss detections also occur that are manually labeled with a yellow cross in sample frames. From the sample frames, it can be seen that a person is effectively detected at several scene locations. However, in some cases, the person's appearance is changing; therefore, the model gives miss detections. The reason for miss detection maybe, as the pre-trained model is applied, and an individual's appearance from an overhead view is changing, which may be misleading for the model.

4.2. Results of social distance monitoring using transfer learning

The transfer learning methodology is applied to improve the accuracy of the detection model. Using an overhead data set, the model is additionally trained using 500 sample frames. The epoch size 40 and batch size 64 is set for training of the model. The training loss and accuracy curves are shown in Figs. 10 and 11 . A new layer is obtained after training the model; that is further appended with a pre-trained model.

The model is now tested for the same test video sequences, as discussed in the above sub-section. The experimental findings reveal that transfer learning significantly increases the detection results, as seen in Fig. 12. From the sample images, it can be visualized that the model detects the individuals at various scene locations. People with various characteristics are effectively-identified, and the social distance between people is also computed, as shown in the sample frames. In sample frames of Fig. 12(a)–(c), there is no social distance violation found, since

Table 1
Comparison results of YOLOv3 with other deep learning models.

S. no.	Model	True detection rate	False detection rate
1.	Fast-RCNN (pre-trained)	90%	0.7%
2.	Faster-RCNN (pre-trained)	92%	0.6%
3.	Mask-RCNN (pre-Trained)	92%	0.5%
4.	YOLOv3 (pre-trained)	92%	0. 4%
5	YOLOv3 (trained overhead data set)	95%	0.3%

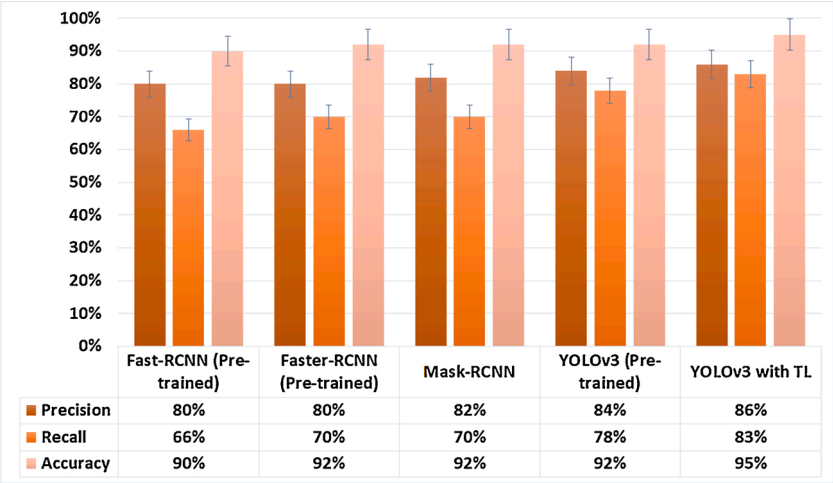

	Fast-RCNN (Pre-trained)	Faster-RCNN (Pre-trained)	Mask-RCNN	YOLOv3 (Pre-trained)	YOLOv3 with TL
Precision	80%	80%	82%	84%	86%
Recall	66%	70%	70%	78%	83%
Accuracy	90%	92%	92%	92%	95%

Fig. 15. Comparison results of YOLOv3 trained on overhead data set with other methods.

all people are marked with green rectangle boxes by the automated framework. While in the sample frame Fig. 12(e), the violation is detected; however, the number of people present in the scene is small as compared to Fig. 12(b), where all people are maintaining social distance, and therefore not a single violation is observed. In Fig. 12(d)–(f), due to close interactions between people, violation is recorded by automated system. The same behavior can be found in Fig. 12(g)–(i) where people are around dozen in both (g) and (h) and violation in (h) is three times as compared to (g). In Fig. 12(d)–(f), multiple people are walking, and entering in the scene are detected and monitored. The framework effectively detected the breach of social distance between people and marked the bounding box as red rectangles if people are too close to each other.

4.3. Performance evaluation

Different quantitative metrics are used in this work to evaluate the performance of the framework for social distance monitoring using a deep learning model and an overhead perspective. To assess the efficiency of the detection model, Precision, Recall, and Accuracy is used. Furthermore, the findings are also compared with other deep learning models. For estimation of Precision, Recall and Accuracy, we used, tp true positive, fp, false positives, tn true negative and fn false-negative. The Accuracy Recall and Precision results are shown in Fig. 13. It can be analyzed that when the model is additionally trained for overhead view data set, the overall performance of the detection model is improved. The tracking accuracy is also given in Fig. 14.

We also compared the newly trained YOLOv3 with other deep learning models. The True detection and False detection rate of different deep learning models are depicted in Table 1. From the results, it can be seen that transfer learning improved the results significantly for the overhead view data set. The false detection rate of different deep learning models are very small, about 0.7–0.4% without any training, which reveals the effectiveness of deep learning models. Different pre-trained object detection models are tested on the overhead data set. Although the models were trained on the different frontal data sets, they still show good results by achieving an accuracy of 90%. In Fig. 15, the comparison results of different state of the art detection are shown.

5. Conclusion and future works

In this work, a deep learning-based social distance monitoring framework is presented using an overhead perspective. The pre-trained YOLOv3 paradigm is used for human detection. As a person's appearance, visibility, scale, size, shape, and pose vary significantly from an overhead view, the transfer learning method is adopted to improve the pre-trained model's performance. The model is trained on an overhead data set, and the newly trained layer is appended with the existing model. To the best of our knowledge, this work is the first attempt that utilized transfer learning for a deep learning-based detection paradigm, used for overhead perspective social distance monitoring. The detection model gives bounding box information, containing centroid coordinates information. Using the Euclidean distance, the pairwise centroid distances between detected bounding boxes are measured. To check social distance violations between people, an approximation of physical distance to the pixel is used, and a threshold is defined. A violation threshold is used to check if the distance value violates the minimum social distance set or not. Furthermore, a centroid tracking algorithm is used for tracking peoples in the scene. Experimental results indicated that the framework efficiently identifies people walking too close and violates social distancing; also, the transfer learning methodology increases the detection model's overall efficiency and accuracy. For a pre-trained model without transfer learning, the model achieves detection accuracy of 92% and 95% with transfer learning. The tracking accuracy of the model is 95%. The work may be improved in the future for different indoor and outdoor environments. Different detection and tracking algorithms might be used to help track the person or people who are violating or breaches the social distancing threshold.

Conflict of interest

None declared.

Declaration of Competing Interest

The authors report no declarations of interest.

Acknowledgments

This work is partially supported by FCT/MCTES through national funds and when applicable co-funded EU funds under the project UIDB/50008/2020; and by Brazilian National Council for Scientific and Technological Development (CNPq) via Grant No. 309335/2017-5.

References

Adlhoch, C. (2020). https://www.ecdc.europa.eu/sites/default/files/documents/covid-19-social-distancing-measuresg-guide-second-update.pdf.
Adolph, C., Amano, K., Bang-Jensen, B., Fullman, N., & Wilkerson, J. (2020). *medRxiv*.

Ahmad, M., Ahmed, I., Ullah, K., Khan, I., & Adnan, A. (2018). *2018 9th IEEE annual ubiquitous computing, electronics mobile communication conference (UEMCON)* (pp. 746–752). https://doi.org/10.1109/UEMCON.2018.8796595

Ahmad, M., Ahmed, I., Ullah, K., Khan, I., Khattak, A., & Adnan, A. (2019). *International Journal of Advanced Computer Science and Applications, 10*. https://doi.org/10.14569/IJACSA.2019.0100367

Ahmad, M., Ahmed, I., Khan, F. A., Qayum, F., & Aljuaid, H. (2020). *International Journal of Distributed Sensor Networks, 16*, 1550147720934738.

Ahmed, I., & Adnan, A. (2017). *Cluster computing* (pp. 1–22).

Ahmed, I., Ahmad, A., Piccialli, F., Sangaiah, A. K., & Jeon, G. (2018). *IEEE Internet of Things Journal, 5*, 1598–1605.

Ahmed, I., Ahmad, M., Nawaz, M., Haseeb, K., Khan, S., & Jeon, G. (2019a). *Computer Communications, 147*, 188–197.

Ahmed, I., Din, S., Jeon, G., & Piccialli, F. (2019b). *IEEE Internet of Things Journal*.

Ahmed, I., Ahmad, M., Adnan, A., Ahmad, A., & Khan, M. (2019c). *International Journal of Machine Learning and Cybernetics*, 1–12.

Ainslie, K. E., Walters, C. E., Fu, H., Bhatia, S., Wang, H., Xi, X., et al. (2020). *Wellcome Open Research, 5*.

B. News (2020). Online. https://www.bbc.co.uk/news/world-asia-china51217455, (Accessed 23 January 2020).

Brunetti, A., Buongiorno, D., Trotta, G. F., & Bevilacqua, V. (2018). *Neurocomputing, 300*, 17–33.

Chakraborty, B. A. (2021). *Springer*.

Chakraborty, C., Banerjee, A., Garg, L., & Coelho Rodrigues, J. J. P. (2021). *Series Studies in Big Data, 80*, 98–136. https://doi.org/10.1007/978-981-15-8097-0

Choi, J.-W., Moon, D., & Yoo, J.-H. (2015). *ETRI Journal, 37*, 551–561.

Ferguson, N. M., Cummings, D. A., Cauchemez, S., Fraser, C., Riley, S., Meeyai, A., et al. (2005). *Nature, 437*, 209–214.

Girshick, R. (2015). *Proceedings of the IEEE international conference on computer vision* (pp. 1440–1448).

Girshick, R., Donahue, J., Darrell, T., & Malik, J. (2014). *Proceedings of the IEEE conference on computer vision and pattern recognition* (pp. 580–587).

Online. https://www.health.harvard.edu/diseases-and-conditions/preventing-the-spread-of-the-coronavirus (Accessed 18 August 2020).

Harvey, A., & LaPlace, J. (2019). *Megapixels: Origins, ethics, and privacy implications of publicly available face recognition image datasets*.

Iqbal, M. S., Ahmad, I., Bin, L., Khan, S., & Rodrigues, J. J. (2020). *Transactions on Emerging Telecommunications Technologies* (p. e4017).

Krizhevsky, A., Sutskever, I., & Hinton, G. E. (2012). *Advances in neural information processing systems* (pp. 1097–1105).

Lin, T.-Y., Maire, M., Belongie, S., Hays, J., Perona, P., Ramanan, D., et al. (2014). *European conference on computer vision* (pp. 740–755). Springer.

Migniot, C., & Ababsa, F. (2016). *Journal of Real-Time Image Processing, 11*, 769–784.

N. H. C. of the Peoples Republic of China (2020). Online. http://en.nhc.gov.cn/2020-03/20/c78006.htm (Accessed 20 March 2020).

Nguyen, C. T., Saputra, Y. M., Van Huynh, N., Nguyen, N.-T., Khoa, T. V., Tuan, B. M., et al. (2020). *Enabling and emerging technologies for social distancing: a comprehensive survey and open problems*. arXiv:2005.02816.

Patrick, S. P., dos Santos, R. S., & de Souza, L. B. M. (2020). In *22nd International Conference on E-Health Networking, Applications and Services (IEEE Healthcom 2020)*.

Pouw, C. A., Toschi, F., van Schadewijk, F., & Corbetta, A. (2020). *Monitoring physical distancing for crowd management: Real-time trajectory and group analysis*. arXiv:2007.06962.

Prem, K., Liu, Y., Russell, T. W., Kucharski, A. J., Eggo, R. M., Davies, N., et al. (2020). *The Lancet Public Health*.

Punn, N. S., Sonbhadra, S. K., & Agarwal, S. (2020a). *medRxiv*.

Punn, N. S., Sonbhadra, S. K., & Agarwal, S. (2020b). *Monitoring COVID-19 social distancing with person detection and tracking via fine-tuned YOLO v3 and Deepsort techniques*. arXiv:2005.01385.

Ramadass, L., Arunachalam, S., & Sagayasree, Z. (2020). *International Journal of Pervasive Computing and Communications*.

Redmon, J., Divvala, S., Girshick, R., & Farhadi, A. (2016). *Proceedings of the IEEE conference on computer vision and pattern recognition* (pp. 779–788).

Redmon, J., & Farhadi, A. (2018). *YOLOv3: An incremental improvement*. arXiv:1804.02767.

Ren, S., He, K., Girshick, R., & Sun, J. (2015). *Advances in neural information processing systems* (pp. 91–99).

Robakowska, M., Tyranska-Fobke, A., Nowak, J., Slezak, D., Zuratynski, P., Robakowski, P., et al. (2017). *Disaster and Emergency Medicine Journal, 2*, 129–134.

Sathyamoorthy, A. J., Patel, U., Savle, Y. A., Paul, M., & Manocha, D. (2020). *COVID-robot: Monitoring social distancing constraints in crowded scenarios*. arXiv:2008.06585.

Simonyan, K., & Zisserman, A. (2014). *Very deep convolutional networks for large-scale image recognition*. arXiv:1409.1556.

Online. https://www.statista.com/chart/21198/effect-of-social-distancing-signer-lab/ (Accessed 18 August 2020).

Szegedy, C., Liu, W., Jia, Y., Sermanet, P., Reed, S., Anguelov, D., et al. (2015). *Proceedings of the IEEE conference on computer vision and pattern recognition* (pp. 1–9).

W. C. D. C. Dashboard (Online). https://covid19.who.int/ (Accessed 23 August 2020).

W.H. Organization (2020). https://www.who.int/emergencies/diseases/novel-coronavirus-2019 (Accessed 02 May 2020).

WHO (Online). https://www.who.int/dg/speeches/detail/2020 (Accessed 12 March 2020).

Yang, D., Yurtsever, E., Renganathan, V., Redmill, K. A., & Özgüner, Ü. (2020). *A vision-based social distancing and critical density detection system for COVID-19*. arXiv:2007.03578.

Yash Chaudhary, D. G., & Mehta, M. (2020). In *22nd international conference on E-health networking, applications and services (IEEE Healthcom 2020)*.